The Effect of Shear Stress and Stretch on Lymphatic Endothelial Cell Calcium Dynamics using a Microfluidic platform

Laboratory of Lymphatic Biology and Bioengineering (LLBB)
School of Mechanical Engineering
Georgia Institute of Technology

Stephen Arjanto
Fall 2017

Introduction

The cardiovascular system is the main transportation pathway in the human body. As blood travels through the body, it delivers oxygen and essential nutrients to the surrounding tissues, some of which are left in the interstitial space outside the blood vessel. This excess water and nutrients are transported back to the circulatory system through the lymphatic system [9].

As stated in Swartz' review article (2001), the lymphatic system consists of the capillaries, collecting vessels, lymph nodes, trunks, and ducts. The capillaries are made of one endothelial cell layer with very few tight cell junctions in the basement membrane. Fluid in the capillaries then proceed to the collecting vessels, which have Smooth Muscle Cells (SMCs) and valves to prevent the fluid from flowing back. Collecting vessels then pass through several nodes. Lymphatic trunks then drain the lymph from the nodes into the ducts, which will empty to the vein [14].

Understanding the response of Lymphatic Endothelial Cells (LECs) to various shear stress and stretch is crucial to know the underlying mechanism of various lymphatic-related diseases, such as lymphedema. Lymphedema is the accumulation of lymph in the body tissue caused by lymph vessel disorder. Hayes et al (2008) and Togawa et al (2014) show that lymphedema affects about 30% of breast cancer survivors, and the incident rate increases with the number of lymphatic nodes removed. In lymphedema, it has been shown that there is an increase of shear stress and stretch experienced by the lymphatic vessel [12]. An in-vivo experiment conducted by Rahbar et al. shows that lymphatic vessels response to edemagenic stress are marked by shear stress increase and higher contraction frequency. To date, no research has been done to assess the Lymphatic Endothelial Cells (LECs) shear stress threshold change in relation to the applied strain. This research objective is to observe the calcium dynamic response

of cultured Lymphatic Endothelial Cells (LECs) exposed to shear stress and stretch in an in-vitro microfluidic platform.

Background

The lymphatic system serves several purposes in the body. First, the lymphatic system transports back the excess nutrients in the tissue space outside the blood vessel. As blood travels through the body, it delivers oxygen and essential nutrients to the surrounding tissues. This nutrient delivery can be achieved due to the presence of leaky junctions among the cells in the capillary blood vessel and the Starling forces across it [8]. As blood continue its circulation back to the vein, some of these nutrients and water is left in the interstitial space outside the blood vessel. This excess water and nutrients are transported back to the circulatory system through the lymphatic system [9]. Second, the lymphatic system also functions as the body's defense system against various infections and diseases. When an infection happens in the body, the bacteria that gets into the tissue space outside blood vessel will eventually be drained into the lymphatic system, in which the lymphocytes will eliminate the infecting agent when passing the lymph node [1]. The third function of the lymphatic system is fat adsorption. When fat is absorbed by the smooth intestine, their molecules are arranged as chylomicrons, Low Density Lipoprotein (LDL), Intermediate Density Lipoprotein (IDL), and High Density Lipoprotein (HDL). These fat structures are absorbed by the lymphatic vessel and transported back to the blood vessel [4].

Recent developments of organ-on-chip technology has enabled researchers to simulate the physiological environment of the body in in-vitro condition. The utilization of microfabrication techniques commonly used in semiconductor industries enables the chip to be fabricated with very high precision, which is especially useful for biomedical research simulating in-vivo condition [13]. The microfluidic device that is used for this study is made from

Polydimethylsiloxane (PDMS). The device itself has three channels, two of them are used to apply vacuum pressure to the main channel in the middle. The flow channel itself is separated into an upper and lower channel by a PDMS membrane, on top of which the cells will be cultured (See Fig. 1).

The shear stress is applied by varying endothelial basal medium (EBM) flowrates in the microfluidic channels. Imposing dynamic shear stress is necessary to simulate the LECs varying shear stress exposure experienced in in-vivo condition. LECs have been shown to be sensitive to shear stress. This response can be observed from the calcium level inside the cell [5]. Jafarnejad shows that when shear stress is applied, the calcium concentration inside the cell increases until it peaks, which will be followed by a drop to the initial basal condition or to a lower condition. The authors note that the first peak is particularly sensitive to shear stress magnitude. When the shear stress is applied for the second time, the peak is lower, indicating that the cell needs some time to replenish the calcium supply and is not as magnitude sensitive.

The cell stretching process is applied by adjusting pressure in the air channels alongside the cell-containing channel of the microfluidic device. The vacuum will be created by using syringe pump controlled by LabVIEW. Physiologically, stretching of LECs correlates to transmural pressure across the walls of the lymphangion [2]. An elevated transmural pressure will result in the stretch of the endothelial cells. Isolated lymphatic vessel with elevated transmural pressure shows an increased wall shear threshold and is capable of synchronizing its pumping action to the imposed flow pressure [6]. Kornuta's paper also highlights that the synchronizing action of the vessel is dependent upon the endothelial cells. As shown in this paper, an isolated lymphatic vessel which has been stripped of its endothelial cell exhibits lower contraction magnitude compared to the vessel where the endothelium is still intact.

Quick et al [10,11] show that lymphatic vessels are capable of acting as a conduit or a pump depending upon the circumstances. When the pressure is higher in the outlet compared to the inlet, the vessel acts as a pump, whereas when the pressure in the outlet is lower than the inlet, the vessel acts as a conduit. This pump or conduit behavior is dependent upon which role requires the least energy [3]. Kunert et al. (2015) also show that endothelial cells have Ca2+ ion channels that are sensitive to mechanical stresses, further underlining the findings in Kornuta's paper. The calcium dynamics of endothelial cells are dependent upon the stretch experienced by the cells itself due to the presence of ion channels on the surface of the cells. These dynamics, in turn, influence the contractility of the lymphatic vessel and determine whether the lymph vessel acts as a pump or a conduit.

This research will potentially advance the understanding of the role lymphatic endothelial cells have in the lymphatic vessel and will serve as a groundwork for future research. Understanding the calcium dynamics of LECs will further the understanding of LECs adaptation mechanism to the higher stretch and shear load during lymphedema development and enable the development of diagnostic and therapeutic technology for various lymphatics related diseases.

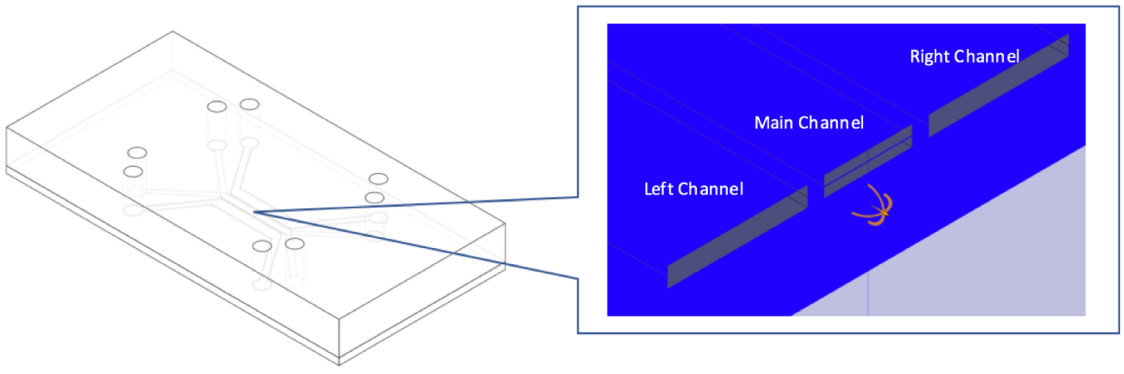

Fig. 1 A three-dimensional view of the microfluidic chip with the stretchable membrane. The thin blue line in the main channel shown in the close-up image is the membrane with embedded fluorescent membrane. The right most and left most channels are the air channel, in which the low pressure is applied. The top channel in the middle is where the LECs are cultured.

Methods

Device fabrication

PDMS (Corning) was mixed with curing agent (15:1) with a final volume of 40 ml and poured to the silicon wafer. The solution was then degassed to remove air bubbles and cured in 60^{o}C oven overnight. The resulting PDMS slab was then cut to form the top part of the device and a biopsy punch (2mm) was used to form the circular inlet and outlet holes. The same procedure was repeated with a final mixture volume of 10 ml to obtain the bottom part of the device. To fabricate the membrane, 10ul of fluorescent bead solution and 1 ml of 20:1 PDMS and curing agent mixture was poured on top a polystyrene dish, and spun at 6000 rpm for 30s. The polystyrene dish was then left in the oven overnight.

After curing, all the PDMS parts were left to cool to room temperature. Then the polystyrene dish was bonded to the top part of the PDMS slab, cut and peeled to separate from the polystyrene dish. The top-membrane part was then bonded to the bottom part and the assembled PDMS part was cured in the oven overnight.

Eight syringe tips were attached to the device and secured with silicone glue. The device was placed in 60^{o}C oven until the glue is fully cured. The device was sterilized by flowing 70% ethanol through all the channels and submerged in 70% ethanol for 10 minutes. The device was dried and kept in the sterile laminar hood.

Cell culture

T25 flask was coated with collagen (Type 1 Rat collagen, 50ug/ml) and incubated at 37^{o}C for one hour, and rinsed with Phosphate-Buffered Saline (PBS) solution prior to putting the LECs to the flask. The cell media was changed once every 24 hours after seeding until cells were at least 90 percent confluent (usually 3 days after seeding). Once the cells were confluent, trypsin

solution was used to detach the cells from the flask and the cell solution was centrifuged at 0.8 Relative Centrifugal Force (RCF) for 5 minutes at 4^{o}C. The supernatant liquid was removed and the cell pellet re-suspended in 2 ml media solution. The new cell solution was then seeded to the top part of the middle channel in the microfluidic device. Prior to cell seeding, the microfluidic device was sterilized by flowing 70% ethanol through the device, rinsed with PBS, and then coated with fibronectin (7.5ug/ml) and left in the incubator for one hour.

After culturing the cells for 24 hour in the microfluidic device under static condition, several images of the cells were taken, and the cells were cultured under constant shear stress of 1 dyne/cm^2 for the subsequent 24 hours. Syringe pump (Genie Touch Syringe Pump – Kent Scientific) and 60ml syringe tube were used to apply the constant shear stress by setting the pump to flow 0.9ml/hr.

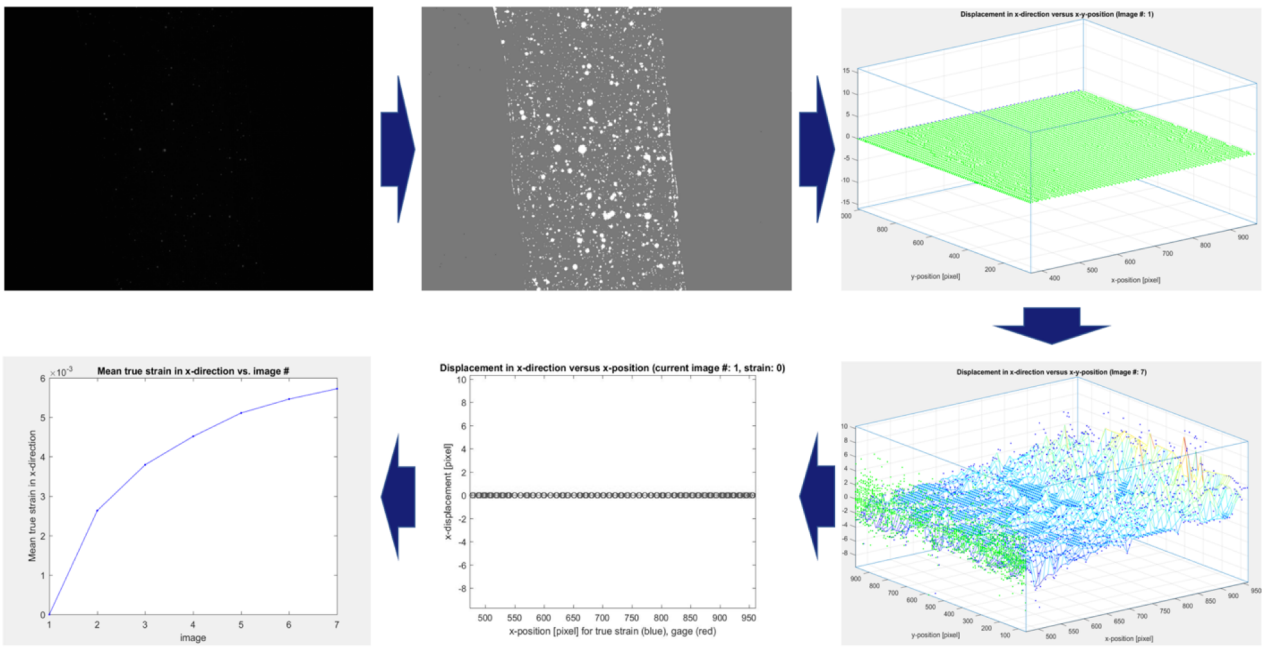

Fig. 2 Schematic of device characteristic process.

Device Characterization

Five devices were tested by applying vacuum to both air channels using syringe pump. The syringe pump was controlled via a custom-build LabVIEW interface which can send stepping command to the pump. Five seconds following the pressure step, the membrane was imaged using the fluorescent Cy-5 lamp. The image sequence obtained from the procedure are then analyzed in MATLAB by using a Digital Image Correlation (DIC) algorithm (Fig. 2).

Calcium Dynamics Analysis

Following the constant flow culture, the cell channel was rinsed with pre-warmed PBS and DMEM/F12. A Fluoro-4 solution was then flowed into the channel and incubated for one hour. Subsequently, the channel was rinsed again using DMEM/F12.

Zeiss inverted microscope with benchtop incubator was used to image the calcium dynamics. The benchtop incubator was set at 37^{o}C with 5% CO_2 concentration. For the shear stress experiment, the cells were imaged under a static condition with an exposure time of 500ms using the Micro-Manager software (UCSF) for one minute, and then imaged under oscillatory shear stress (Amplitude = 1 dyne/cm2, frequency = 0.133 Hz, Offset = 0.5 dyne/cm2) for 5 mins. In the strain experiment, the cells were imaged at no strain for one minute and under strain for another 3 minutes.

Multiple regions of interests (ROIs) were selected by importing the image sequence to ImageJ. The measurement file was then exported as a .csv file and analyzed further using MATLAB (Natick, MA). The normalized intensity plot of each ROI was plotted against the image number multiplied by the exposure time in seconds to show the real experiment time.

Results

Device Characterization

The following table shows more detailed numerical magnitude of the device strain under applied vacuum. A total of 5 devices were used in the characterization process.

Table 1 – Microfluidic Device Characterization		
Pressure (atm)	Mean Engineering Strain	Standard Deviations
1	0.0000000E+00	0
0.64884993	5.0938774E-03	0.001725711
0.480220476	7.5896174E-03	0.002567086
0.38116071	8.8606868E-03	0.002824525
0.315980357	9.6524321E-03	0.003181247
0.269836919	9.4900366E-03	0.002872989
0.235453088	9.8902287E-03	0.003061768
0.20884156	1.0458969E-02	0.003395921

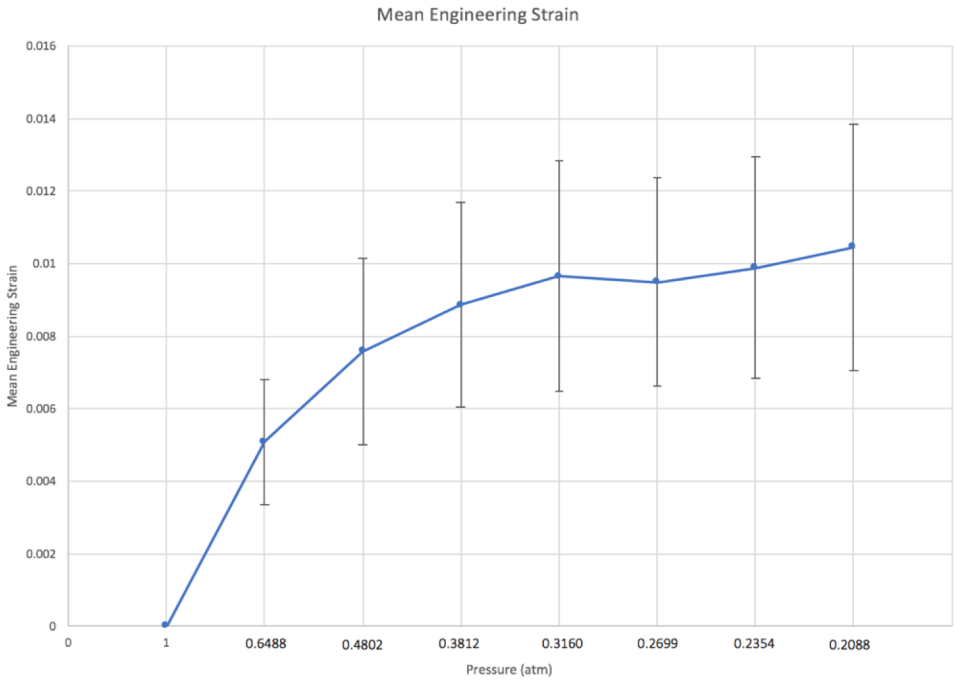

Fig. 3 Average mean engineering strain of the device. N = 5 devices. Vertical bars represent standard deviations. The result is obtained from MATLAB DIC Algorithm.

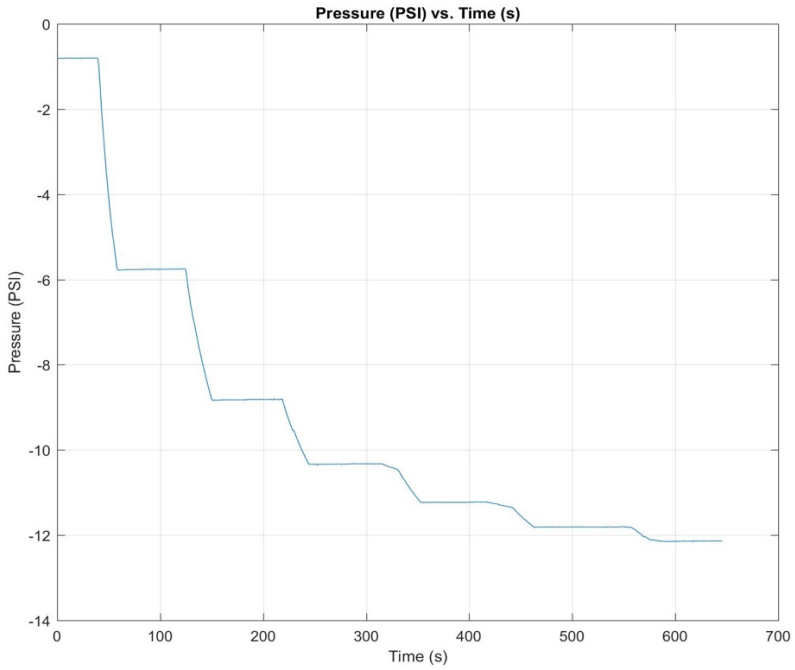

Fig. 4 Pressure graph for checking the device ability to hold pressure. A syringe pump is used to create low pressure in the side channels of the device. A step pressure is applied to the device and held for about one minute for each step. The relatively flat pressure values on each step shows that the device can maintain the applied pressure (no leakage).

Calcium Dynamics Experiment

Multiple ROIs were manually selected in ImageJ and the data inputted into MATLAB. Each ROI was chosen such that it only includes one cell per ROI while minimizing the background of the cell. To obtain the background image, an area of the image which was not near the cells and did not have significant noise (e.g. Fluoro-4 particles or detached cells going through the ROI) was chosen and its mean data was used for data processing.

For the shear strain experiment, the cells were imaged under static condition for one minute, followed by sinusoid shear stress (Amplitude = 1dyne/cm2, offset = 0.5 dyne/cm2, frequency = 0.133 Hz – frequency is based on Zawieja (2009) finding) was applied to the cells and its images taken. Figure 5 shows normalized intensity values for the four experiments conducted to assess the cells' calcium dynamics in response to shear stress. To normalize the

data, each cells ROI average was subtracted by the average of the background ROI average, and then divided by the maximum value obtained from the subtraction. The absolute of the minimum value was then added to the intensity value to keep all the intensity values positive.

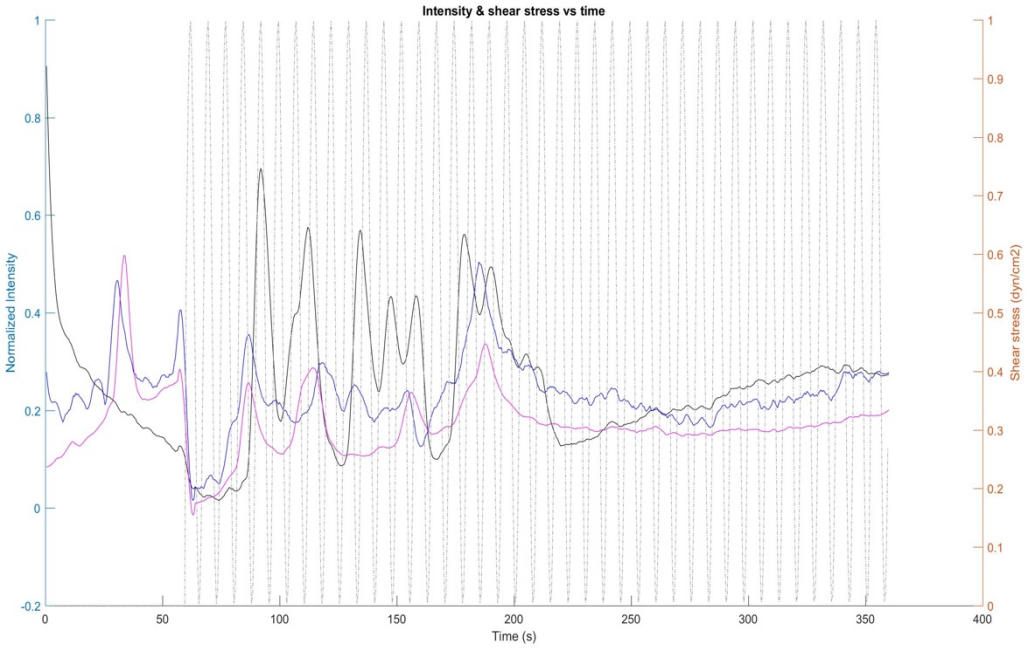

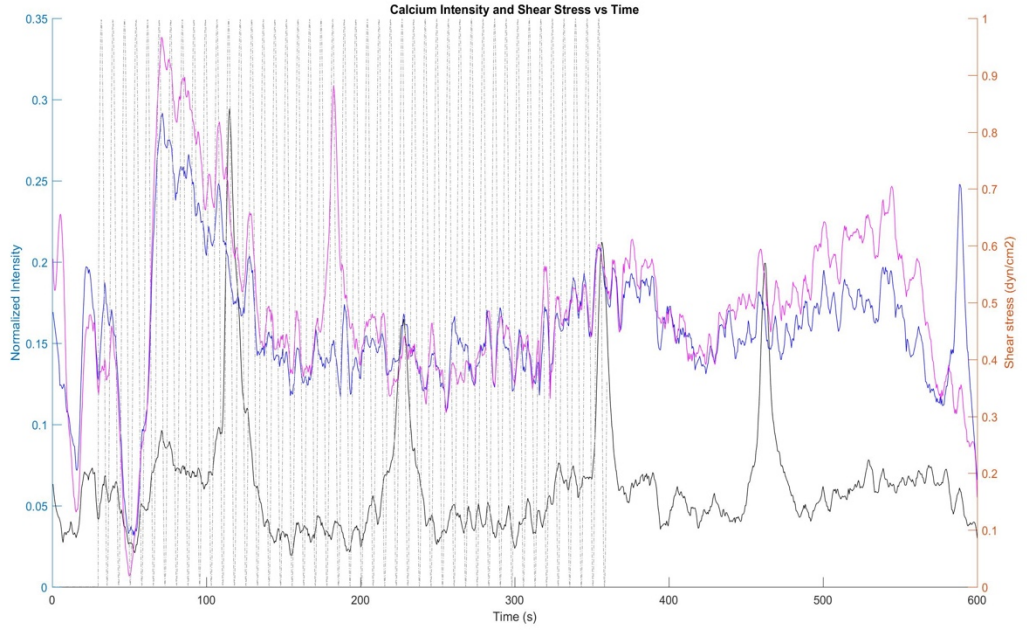

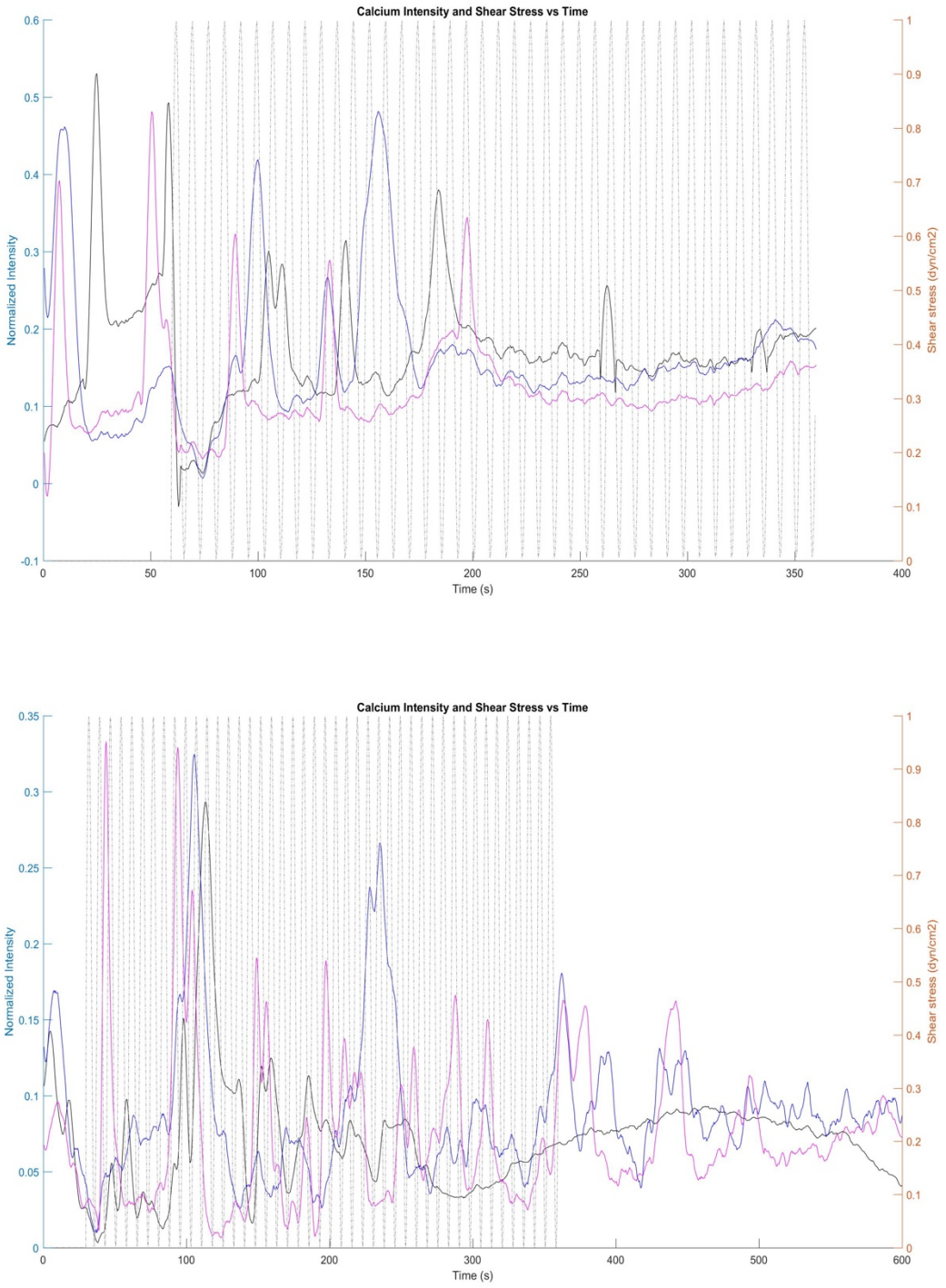

Fig. 5 Lymphatic Endothelial Cells Calcium Dynamics Under Oscillatory Shear Stress. Zeiss inverted microscope with benchtop incubator was used to image the calcium dynamics. The incubator is set at 37^{o}C with 5% CO_2 concentration. Exposure time was set at 500ms and shear stress is 1 dyne/cm2. The shear stress is applied by flowing DMEM/F12 to the channels using a syringe pump controlled by a LabVIEW VI.

For the strain experiment, cells were cultured on the top of the membrane for 24 hours. The cells were then sheared under 24 hours to achieve alignment with the flow. The cells were imaged under no strain condition for one minute, followed by three minutes of strained condition.

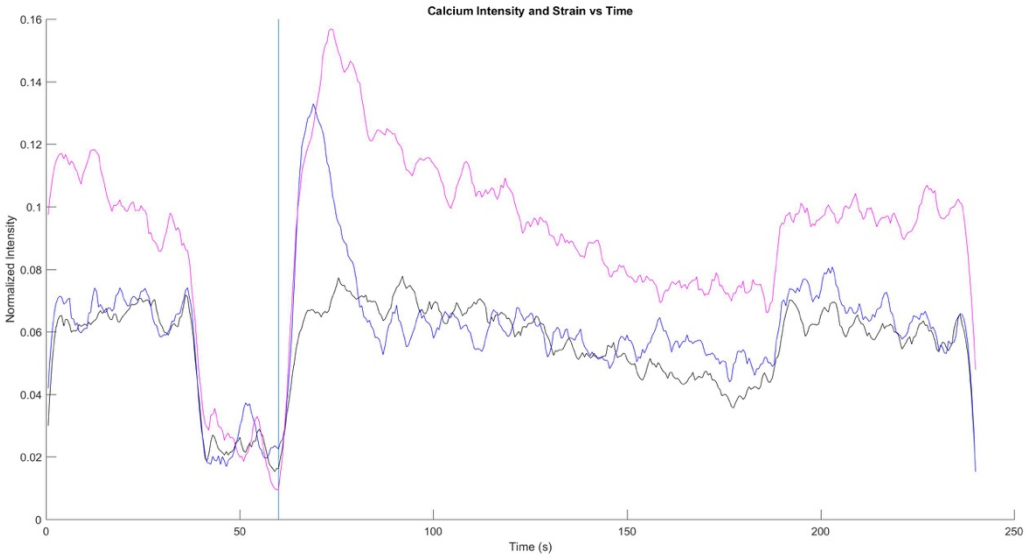

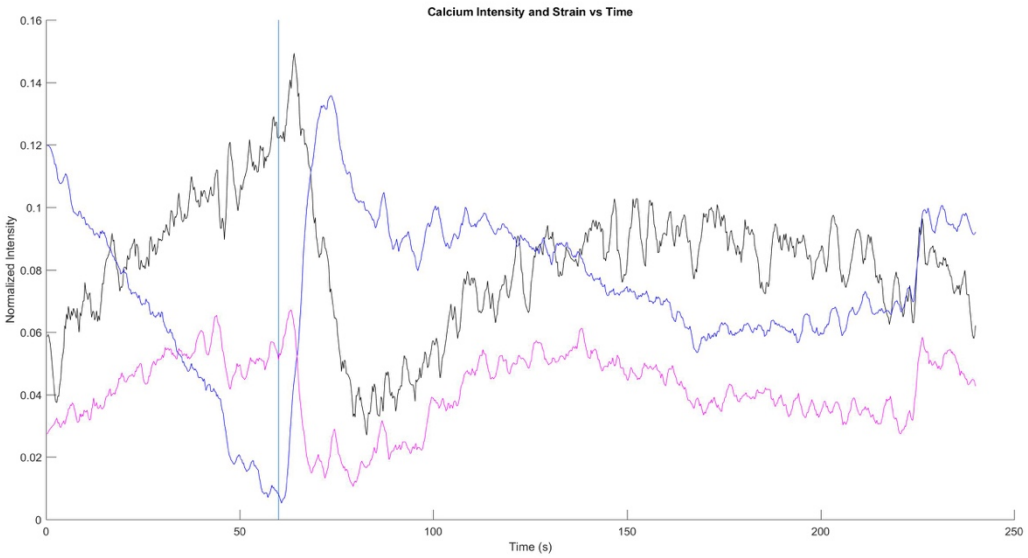

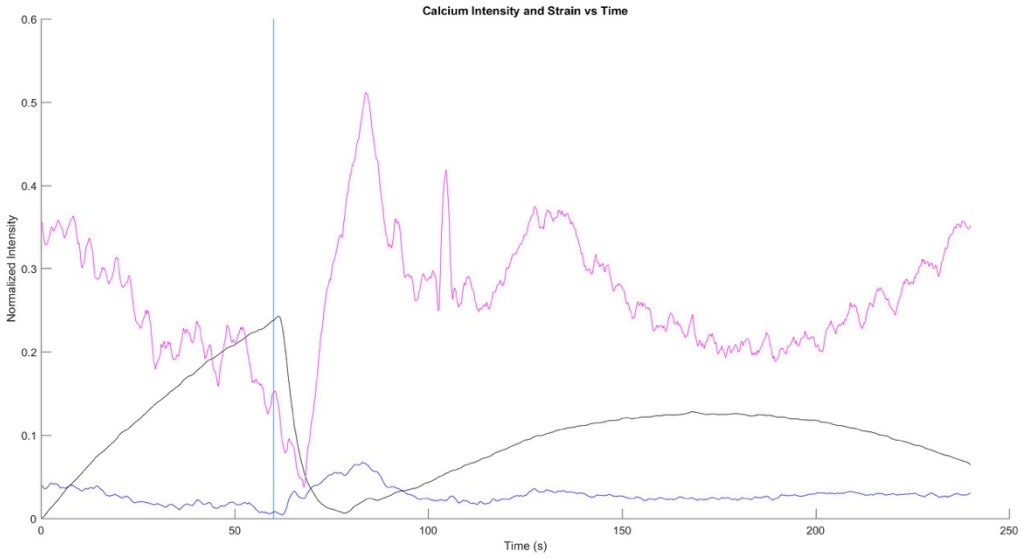

Fig. 6 Lymphatic endothelial cells calcium dynamics under strain. Zeiss inverted microscope with benchtop incubator was used to image the calcium dynamics. The incubator is set at 37^{o}C with 5% CO_2 concentration. Exposure time was set at 500ms. The strain is applied using a syringe pump to create a low pressure in the side channels of the device.

Discussion and Conclusion

The microfluidic device was successfully assembled with respect to its intended purpose, as a platform capable of applying shear stress and strain concurrently. The pressure graph of the device (Fig 4) shows that the device can maintain the low pressure for the length of the experiment, hence pressure leakage is not a concern. The device currently has a maximum strain around 1.2% as calculated by MATLAB DIC Algorithm. There can be multiple reasons that affect the percentage of strain of the device, however, a strong factor might be the membrane was initially a little bit loose and become tight when it was stretched. In future studies, the microfluidic device can be made with thinner walls between the channels, so larger strain can be produced.

The shear stress experiments show that the LECs' calcium dynamic is influenced by the applied shear stress. In all four experiments, the shear stress initiated a calcium dynamic response in the cells.

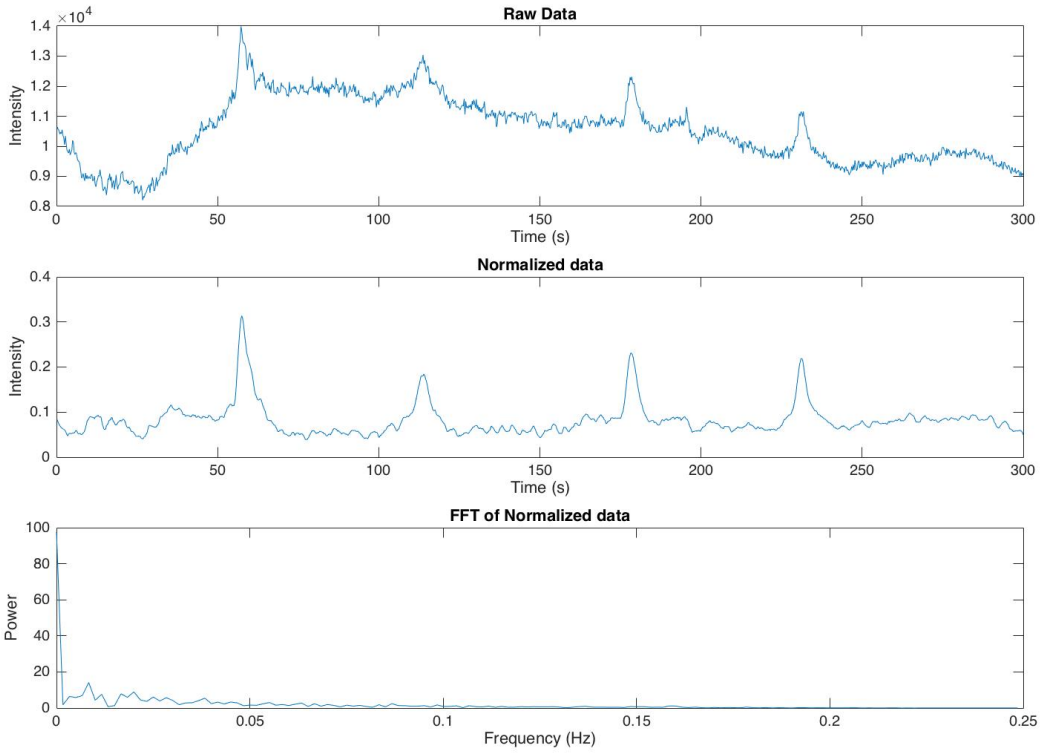

Fig. 7 Illustration of the data analysis process for the calcium dynamic of lymphatic endothelial cells. The raw data, shown on the topmost, is obtained using Zeiss inverted microscope with benchtop incubator set at 37°C and 5% CO_2. Multiple ROIs are then selected in ImageJ and imported as a .csv into MATLAB. The middle graph shows the normalized data. The bottom graph shows the FFT of the normalized data.

For the calcium dynamics shear stress experiment, Fast Fourier Transform (FFT) was used to analyze the frequency content of the calcium dynamics. Fast Fourier transform was performed to the normalized data of the calcium dynamics, and three of the highest power peak and their respective frequency noted (table 2). In the normalization procedure, the data was

filtered using Savitzky-Golay filter to smooth the data. Savitzky-Golay filter was used since the data contains a lot of peaks, and Savitzky-Golay filter preserves the peak location and the peak width while performing the smoothing procedure.

Table 2 - FFT Data

Experiment	Dominant Frequency	Power
I – ROI 4	0.01391	16.37872
	0.02503	12.08521
	0.03338	10.69208
II - ROI 1	0.00834	14.12166
	0.01668	7.86645
	0.02002	8.92208
III – ROI 2	0.00834	19.55257
	0.01501	13.87136
	0.02335	10.09003
III – ROI 3	0.01168	9.03917
	0.01501	13.06303
	0.01835	18.99155
I – ROI 2	0.01336	17.34633
	0.03118	6.87447
	0.04009	7.83300
I – ROI 5	0.01782	13.86420
	0.03563	8.48898
	0.05791	6.44117
IV – ROI 1	0.01336	7.92343
	0.02227	11.54789
	0.04900	8.91951

One of the difficulties that were encountered when trying to analyze the data using FFT was there was no clear way to choose the window size for the FFT. In order to circumvent this problem, a more advanced signal processing method, wavelet transform, was also utilized to analyze the calcium dynamics data.

Table 3 - Wavelet Transform Data		
Experiment	Mean Dominant Freq.	Std. Dev of Dominant Freq.
I – ROI 4	0.0205	0.0033
II - ROI 1	0.0051	0.0007
III – ROI 2	0.0058	0.0011
III – ROI 3	0.0151	0.0021
I – ROI 2	0.0149	0.0033
I – ROI 5	0.0184	0.0017
IV – ROI 1	0.0191	0.0049
Average	0.0141	0.0015

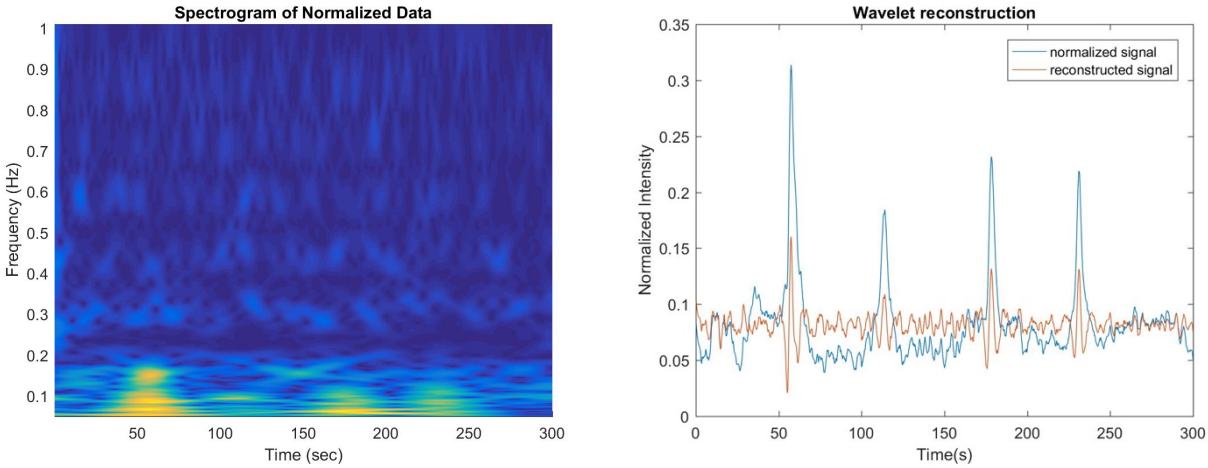

Fig. 8 Wavelet transform of the calcium dynamics signal. The wavelet transform was performed using MATLAB wavelet toolbox. Largest power and its corresponding frequency in the FFT data obtained from the wavelet transform for each experiment were averaged to get the average frequency of the calcium dynamics response (table 3).

The strain experiments show that the applied strain does not cause any oscillatory calcium level change in the cells. There are multiple reasons that may cause this result: First, it might be that the strain applied (about 1.2%) is too low to initiate any response from the cells. Second, it might be caused by the cells morphology – i.e. the cells did not form a fully confluent layer on the membrane when the strain experiment was conducted. The third reason, it is possible that strain does not independently alter the calcium dynamics of lymphatic endothelial

cells. The applied strain might play a role in changing the threshold of the cells' calcium dynamics in response to shear stress.

Future studies

There are several things that can be examined to further understand the effect of strain and shear stress on lymphatic endothelial cells' calcium dynamics. Further research should examine the response of LECs to larger strain. Understanding the response of the cells in strain-only condition will help confirm whether the minimal calcium response shown in this study is caused by low level of strain or that the cell's calcium dynamic is not affected by the application of strain only. The other experiment that should be performed is utilizing ramped shear stress combined with strain. The data gathered from this research highlights the possibility that strain does not independently cause calcium dynamics alteration apart from shear stress. Ramped shear stress should be applied to the cells under no strain and strain condition, and the activation threshold for both cases can be analyzed further. A more advanced feature extraction method, such as wavelet analysis, can also be utilized to better understand the role of strain and shear stress in lymphatic endothelial cells' calcium dynamics.

References

1. Adamczyk, L. A., Gordon, K., Kholova, I., Meijer-Jorna, L. B., Telinius, N., Gallagher, P. J., . . . Baandrup, U. (2016). Lymph vessels: the forgotten second circulation in health and disease. Virchows Arch, 469(1), 3-17. doi:10.1007/s00428-016-1945-6

2. Breslin, J. W. (2014). Mechanical forces and lymphatic transport. Microvasc Res, 96, 46-54. doi:10.1016/j.mvr.2014.07.013

3. Gashev, A. A. (2002). Inhibition of the active lymph pump by flow in rat mesenteric lymphatics and thoracic duct. The Journal of Physiology, 540(3), 1023-1037. doi:10.1113/jphysiol.2001.016642

4. Huang, L. H., Elvington, A., & Randolph, G. J. (2015). The role of the lymphatic system in cholesterol transport. Front Pharmacol, 6, 182. doi:10.3389/fphar.2015.00182

5. Jafarnejad, M., Cromer, W. E., Kaunas, R. R., Zhang, S. L., Zawieja, D. C., & Moore, J. E., Jr. (2015). Measurement of shear stress-mediated intracellular calcium dynamics in human dermal lymphatic endothelial cells. Am J Physiol Heart Circ Physiol, 308(7), H697-706. doi:10.1152/ajpheart.00744.2014

6. Kornuta, J. A., Nepiyushchikh, Z., Gasheva, O. Y., Mukherjee, A., Zawieja, D. C., & Dixon, J. B. (2015). Effects of dynamic shear and transmural pressure on wall shear stress sensitivity in collecting lymphatic vessels. Am J Physiol Regul Integr Comp Physiol, 309(9), R1122-1134. doi:10.1152/ajpregu.00342.2014

7. Kunert, C., Baish, J. W., Liao, S., Padera, T. P., & Munn, L. L. (2015). Mechanobiological oscillators control lymph flow. Proceedings of the National Academy of Sciences Proc Natl Acad Sci USA, 112(35), 10938-10943. doi:10.1073/pnas.1508330112

8. Levick, J. R., & Michel, C. C. (2010). Microvascular fluid exchange and the revised Starling principle. Cardiovasc Res, 87(2), 198-210. doi:10.1093/cvr/cvq062

9. Munn, L. L. (2015). Mechanobiology of lymphatic contractions. Semin Cell Dev Biol, 38, 67-74. doi:10.1016/j.semcdb.2015.01.010

10. Quick, C. M., Venugopal, A. M., Gashev, A. A., Zawieja, D. C., & Stewart, R. H. (2006). Intrinsic pump-conduit behavior of lymphangions. AJP: Regulatory, Integrative and Comparative Physiology, 292(4). doi:10.1152/ajpregu.00258.2006

11. Quick, C. M., Ngo, B. L., Venugopal, A. M., & Stewart, R. H. (2009). Lymphatic pump-conduit duality: contraction of postnodal lymphatic vessels inhibits passive flow. Am J Physiol Heart Circ Physiol, 296(3), H662-668. doi:10.1152/ajpheart.00322.2008

12. Rahbar, E., Akl, T., Cote, G. L., Moore, J. E., Jr., & Zawieja, D. C. (2014). Lymph transport in rat mesenteric lymphatics experiencing edemagenic stress. Microcirculation, 21(5), 359-367. doi:10.1111/micc.12112

13. Skardal, A., Shupe, T., & Atala, A. (2016). Organoid-on-a-chip and body-on-a-chip systems for drug screening and disease modeling. Drug Discov Today, 21(9), 1399-1411. doi:10.1016/j.drudis.2016.07.003

14. Swartz, M. A. (2001, August 23). The physiology of the lymphatic system. Advanced Drug Delivery Reviews, 50(1-2), 3-20. http://dx.doi.org/10.1016/S0169-409X(01)00150-8

15. Togawa, K., Ma, H., Sullivan-Halley, J., Neuhouser, M. L., Imayama, I., Baumgartner, K. B., . . . Bernstein, L. (2014). Risk factors for self-reported arm lymphedema among female breast cancer survivors: A prospective cohort study. Breast Cancer Research Breast Cancer Res, 16(4). doi:10.1186/s13058-014-0414-x